

# LOW-SPEED CONTROL OF TILT-ROTOR AIRCRAFT USING H-INFINITY

D. J. Walker, M. Voskuijl and B. J. Manimala

Engineering Department  
Liverpool University  
Liverpool L69 3GH  
United Kingdom

**Key words:** Tilt-rotor aircraft, control systems, stability augmentation, handling qualities

**Abstract:** The drive to develop a European Civil Tilt Rotor (CTR) aircraft has led to renewed interest and research in Europe into the dynamics, control and handling qualities of this type of aircraft. This paper presents preliminary results from a study into the design of a high-performance stability and control augmentation system for such an aircraft. Central to the study is a high-order non-linear model of the Bell XV-15 aircraft and its control system. Simulation results and analysis are presented giving an indication of the high levels of stability, performance and handling qualities that could potentially be available on a future CTR aircraft in the hover/low-speed part of the flight-envelope, where the unaugmented aircraft exhibits some undesirable characteristics. Some comparisons are made between the H-infinity controller and the Bell XV-15 core SCAS and the results of a piloted simulation are also discussed.

## 1 INTRODUCTION

Tilt-rotor aircraft combine the vertical take-off and landing capabilities of helicopters with the high-speed cruise performance and economy of turboprops. Their potential to fulfill a number of civil and military requirements, ranging from commuter transport to search-and-rescue, is well recognized. Yet at the same time, this class of aircraft exhibit relatively poor stability and handling characteristics, particularly at hover and low-speed: cross-couplings, lightly-damped or unstable modes, and non-minimum phase (i.e. right-half plane) zeros.

As part of a recent European Civil Tilt-rotor (CTR) initiative, several projects have recently been undertaken with the aim of developing various aspects of Tilt-Rotor critical technologies. Handling Qualities (HQs) and structural loads have been amongst the topics investigated; see [1]-[3] and the references therein. In [3], several load alleviation (SLA) control laws were presented for a tilt-rotor in airplane mode. These control laws were designed using  $\mu$ -synthesis and H-infinity optimal control. The aim was to reduce rotor gimbal flap and rotor oscillatory yoke chord bending moment during longitudinal manoeuvring by designing an SLA control law to make adjustments to the elevator and cyclic controls. A fourth-order H-infinity SLA control law achieved attenuation of flap and bending moment in the range 5-15 dBs on simulations of Eurocopter's EURO TILT. Using these modern multivariable control methods, it was possible to trade off load alleviation, control authority and performance in a systematic manner.

The experience designing SLA control laws led us to ask what level of performance might be achievable if similar control design methods were applied to the synthesis of the tilt-rotor's core stability and control augmentation system (SCAS). This paper presents preliminary results from a study aimed at starting to answer that question. Using a high-fidelity simulation model of the Bell XV-15 aircraft [2,3], we design and test a new SCAS for the hover/low-

speed regime. The aim has been to design a feedback system that provides robust stability and performance around hover.

## **2 DESCRIPTION OF THE BASELINE SYSTEM**

### **2.1 XV-15 Aircraft**

The Bell XV-15 is a twin-engined tilt-rotor aircraft with two 25 ft diameter prop-rotors mounted on wingtip nacelles which can be rotated from horizontal to just beyond vertical, allowing the aircraft to convert between aeroplane and helicopter modes while in flight. Two aircraft were built by Bell under a joint NASA / US Army program. The experience gained with the XV-15 has influenced the development of the V-22 and the Bell Agusta 609 civil tilt-rotor. An account of the development, the characteristics and the specifications of this aircraft can be found in [4].

### **2.2 The Nonlinear FXV-15 Model**

The nonlinear model used in this paper was developed for use in earlier studies including [1]-[3] that were part of a European CTR research initiative. More information about the model can be found in [3]. It was created using data from [5] which were programmed into FLIGHTLAB, a proprietary rotorcraft modelling and simulation language. The model, referred to as FXV-15, gives good correlation with the available flight-test data. In addition to its use as a tool for off-line analysis and design, it has been used extensively in various configurations in support of real-time piloted simulations.

The main characteristics of the model are as follow. The aircraft's two 3-bladed counter-rotating gimbal-mounted prop-rotors are modelled as if rigid. The gimbals are modelled with torsional spring-damper components in pitch and roll. No individual blade flapping is modelled in the FXV-15. Instead, gimbal rotational degrees of freedom are present. The prop-rotor blades are further modelled with non-linear, quasi-steady aerodynamics in table look-up form as functions of angle of attack and Mach number, computed on equal-annulus blade segments. A three degree-of-freedom, finite-state rotor inflow model was used. The engine-governor system of the XV-15 was modelled as a simple first-order relationship between output and commanded torque; the latter is a function of throttle setting and atmospheric conditions, with throttle and collective geared together as a function of nacelle tilt. The drive-train was modelled as a collection of gear, drive, clutch and bearing components with the interconnect shaft that connects the two rotors modelled as the single degree of freedom driven by the resultant torque. The interconnect shaft allows power to be transmitted from one engine to both rotors in the event of a single engine-failure and ensures identical rotor speeds during manoeuvres. The wing/flap lift, drag and pitching moment coefficients are defined as functions of angle of attack, nacelle angle and flap setting. Four segments are used, with the outer port and starboard segments immersed in the rotor slipstreams and two inner sections assumed to be unaffected by the rotor wake. Rotor-wing-empennage interaction was modelled by superimposing the uniform component of the rotor induced velocity onto the wing-empennage velocities, with the wing-empennage downwash angle included. In addition, nonlinear fuselage aerodynamics are functions of angle of attack and sideslip; empennage aerodynamics are modelled in a similar manner to the main wing.

The FXV-15 baseline control system replicates the mechanical interlinks between the pilot's controls, the rotor, and the aeroplane-type control surfaces, with gearings set as functions of nacelle angle; the system also includes a three-axis SCAS, with gains scheduled against speed and nacelle angle. The SCAS provides rate damping and feed-forward response quickening.

### 3 FXV-15 OPEN-LOOP CHARACTERISTICS

We begin with a brief description of the dynamics of the aircraft at low speed. The dominant, "classical" open-loop lateral/directional and longitudinal helicopter-like modes are obtained from the non-linear FXV-15 model by trimming and linearization.

At 10 knots, the longitudinal dynamics are dominated by an unstable oscillatory mode with a time-to-double of approximately 4 seconds and a damped natural frequency of 0.43 rad/s. The transfer function from longitudinal cyclic ( $\theta_{1s}$ ) to pitch attitude ( $\theta$ ) also has a zero very close to the origin. (At hover, this zero lies in the right-half plane.) The 10 knot longitudinal transfer function is:-

$$\frac{\theta}{\theta_{1s}} = \frac{-3.78(s+0.003)(s+0.174)}{(s+0.462)(s+0.211)[-0.38, 0.43]} \frac{[\text{deg}]}{[\text{deg}]} \quad (1)$$

in which the notation  $[\zeta, \omega]$  stands for a second-order term of the form  $s^2 + 2\zeta\omega s + \omega^2$ .

The lateral-directional dynamics are characterized by a roll-subsidence-like mode with time-constant of approximately 1.3 seconds, a spiral-like mode with a time-to-double of approximately 10 seconds, and an unstable dutch-roll mode with a time-to-double of approximately 17 seconds. The lateral/directional dynamics are characterized at 10 knots by a transfer function from differential collective ( $\theta_{0d}$ ) to bank angle ( $\phi$ ) of the form

$$\frac{\phi}{\theta_{0d}} = \frac{29.7[0.389, 0.144]}{(s+0.74)(s-0.069)[-0.11, 0.36]} \frac{[\text{deg}]}{[\text{deg}]} \quad (2)$$

Fig. 1 shows the loci of the poles of the transfer functions over the speed range 0-60 knots. Also shown are the boundaries from ADS-33 [6]. From a handling qualities perspective, the stability is border-line Level 1/2 in this regime, dropping to Level 3 at very low speed.

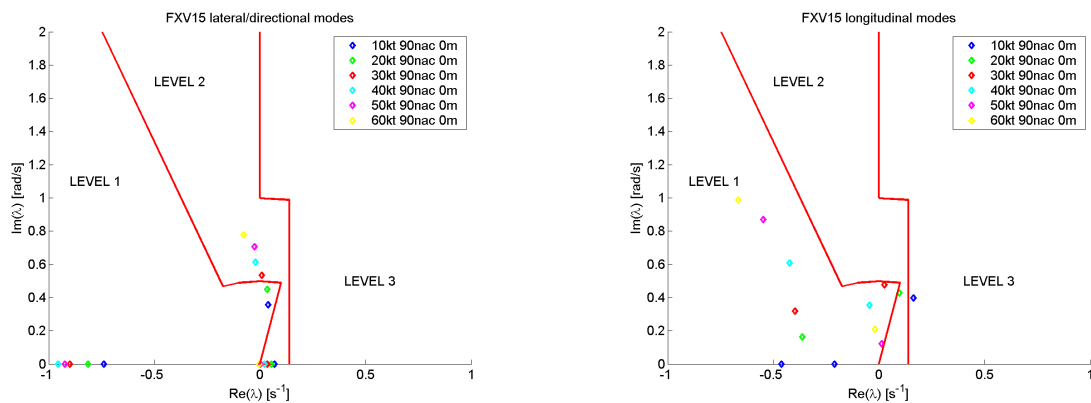


Fig. 1. Open Loop Mid-Term Modes

### 4 CONTROLLER DESIGN FOR HOVER/LOW-SPEED

The 10-knot 90deg nacelle (i.e. helicopter mode) condition was chosen as the nominal design point and the controller was designed to use the helicopter-like controls. The existing SCAS and interlinks were removed so that a totally new approach could be applied to the design of a

control system. In the low-speed regime, control of pitch attitude is through longitudinal cyclic (th1s), as on a conventional helicopter. Roll control is via differential collective (th0d); yaw control is via differential longitudinal cyclic (th1sd). The heave axis was left open-loop. The aim was to stabilize the aircraft and to provide a decoupled attitude command, attitude hold (ACAH) response type in pitch and roll, and a rate command (RC) response type in yaw. Pitch and roll attitudes and roll, pitch, and yaw rates were fed back to the controller. The controller design proceeded essentially along the lines proposed in [7], namely, two separate sub-controllers: one for longitudinal, the second for lateral/directional control. For the design, a high-order linearization of the fully coupled body-rotor dynamics was partitioned into longitudinal and lateral/directional subsystems. The rotor degrees of freedom (relatively high frequency modes) were then removed from the design models. The controller synthesis was based on the H-infinity Loop-Shaping Design Procedure [8]. This is a simple-to-use yet effective optimization. The design procedure works by first cascading the plant with input weights (in this case, simple proportion-plus-integral compensation in each of the three main control loops), then performing a robust stabilization. The resulting lateral/directional and longitudinal controllers were of 8th and 6th order respectively, including the input weights. The controllers were implemented and their reference input channels scaled in such a way as to facilitate limited authority operation, though in this study, no authority limits were imposed. Fig. 2 shows the longitudinal and lateral/directional control loops. The feed-forward path from reference signal to actuator could, in principle, be a mechanical linkage, with the control law dynamics implemented in a fly-by-wire system.

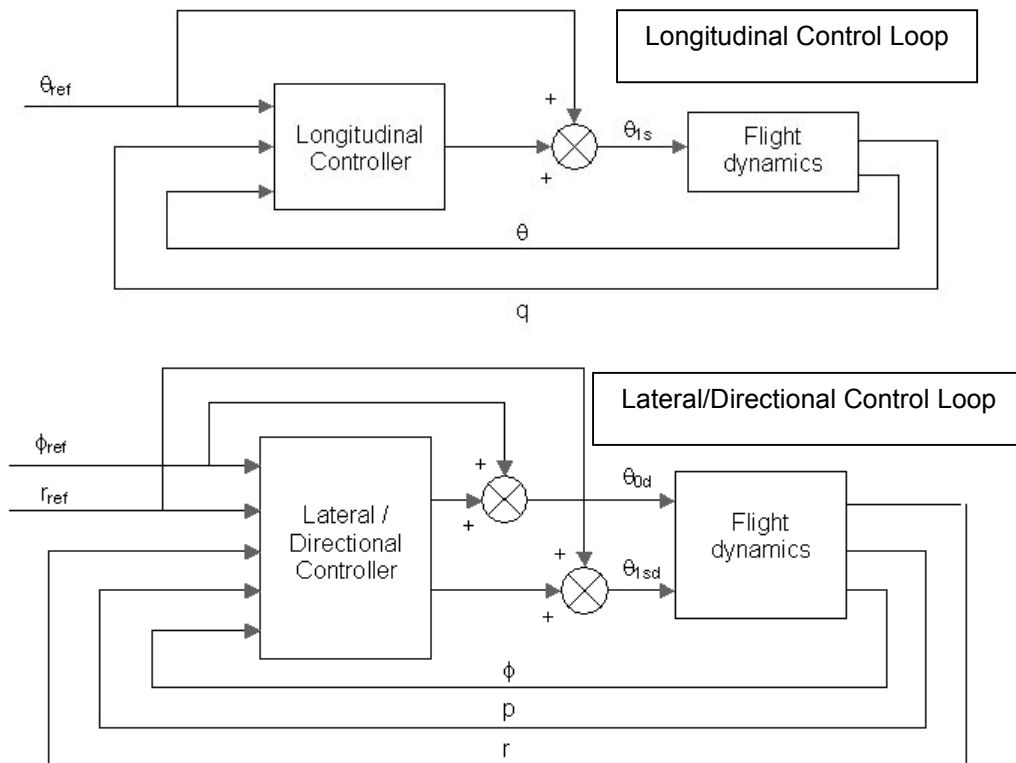


Fig. 2. System Block Diagram

## 5 LINEAR ANALYSIS AND SIMULATIONS

The control system was first tested for stability over the range 10-60kts on the high-order fully coupled linearized model, containing 60 rad/s bandwidth actuator and rotor gimbal

flapping dynamics. Eigenvalue analysis indicated that small-signal stability was achieved over the whole range. The eigenvalues corresponding to the mid-term modes are plotted in Fig. 3 with the HQ boundaries from [6].

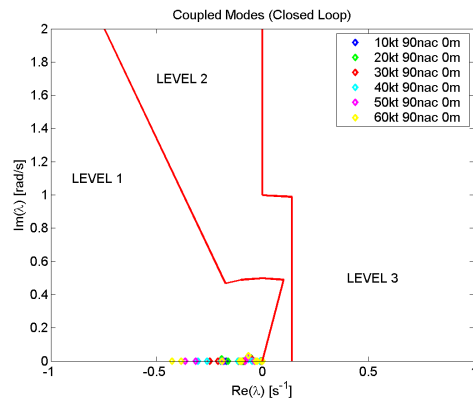


Fig. 3. Coupled Closed-Loop Mid-Term Modes

Pulse inputs were then applied in turn to each of the command axes of the controller, connected to the high-order linearized model. The results obtained for the 10 knot design flight condition are shown in Figs. 4-6. These show the simulated aircraft roll and pitch attitudes (phi and theta respectively) and the yaw rate (r). Also shown are the control variables, i.e. differential collective (th0d), longitudinal cyclic (th1s) and differential longitudinal cyclic (th1sd). The controller has clearly achieved the stabilized ACAH / RC responses types required. Linear simulations away from the design condition showed that the degradation in performance was only slight.

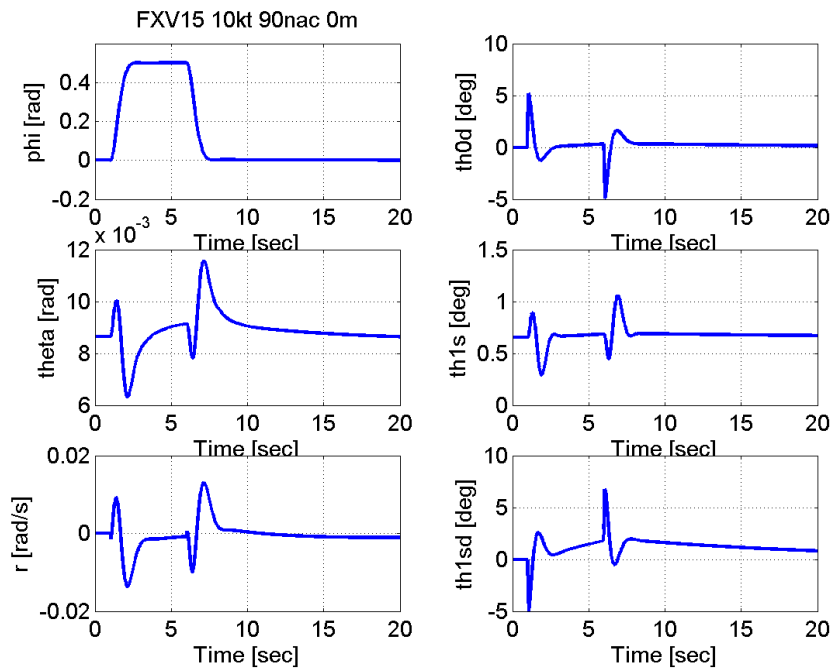


Fig.4. Linear Roll Axis Response: (10kt Design Condition)

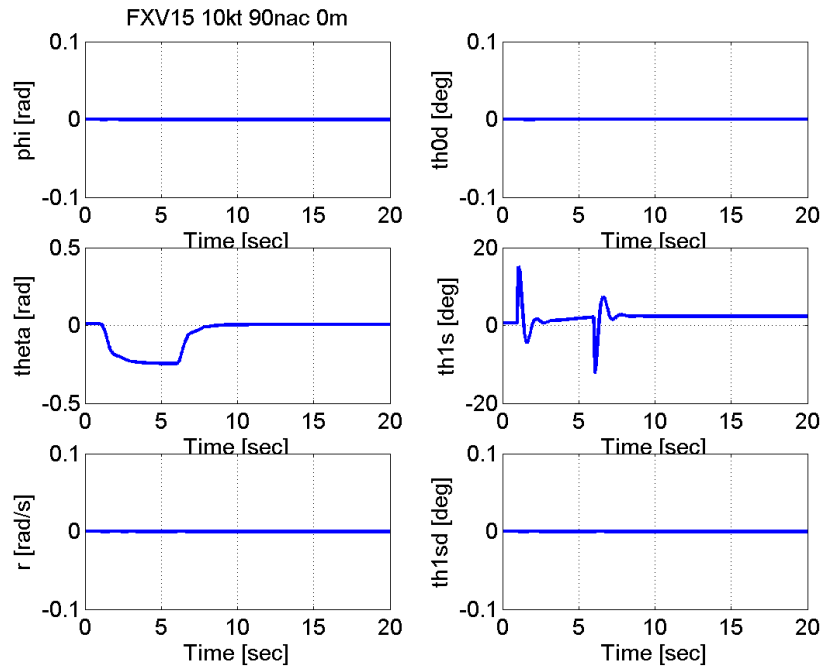


Fig. 5. Linear Pitch Axis Response: (10kt Design Condition)

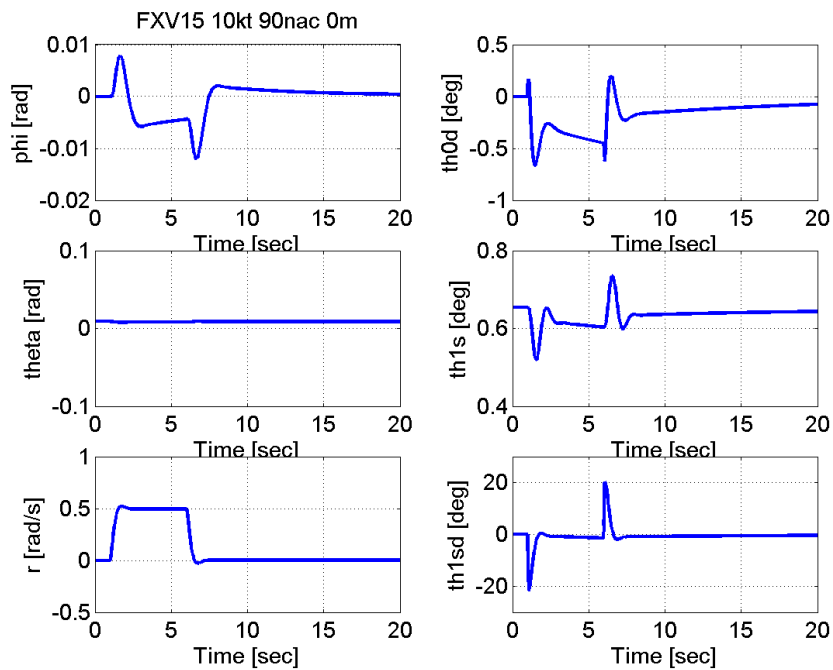


Fig. 6. Linear Yaw Axis Response: (10kt Design Condition)

To give some indication of the difference in behaviour between the H-infinity controller and the XV-15 SCAS, Fig. 7 shows the response to a 3 second pulse of amplitude 1 inch on lateral stick, simulated on the linear XV-15 model at 10kts with the SCAS. The SCAS gives a rate-like response.

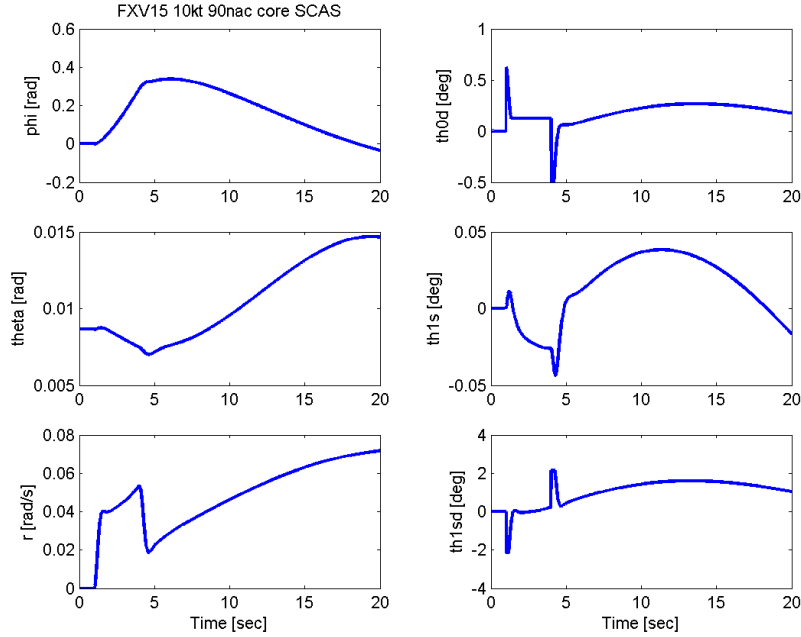


Fig. 7. Roll Axis Response with XV-15 SCAS: (10kt Design Condition, Linear Model)

## 6 FREQUENCY DOMAIN ANALYSIS

### 6.1 Robustness

In addition to performing closed-loop simulations, it is important to assess the robustness properties of the feedback system. A basic analysis has been carried out using the unstructured robustness tests based on the singular values of the input complementary sensitivity and sensitivity functions; see Fig. 8. These tests are based on the Small Gain Theorem, which gives the size of the smallest (in terms of H-infinity norm) perturbation that will destabilize the feedback loop. The following conservative bounds on the MIMO margins can be computed. First, the size of the smallest destabilizing input multiplicative unstructured uncertainty

$$\|\Delta_{\min}\|_{\infty} = 1/1.53 (= 65\%)$$

Second, using formulae from [9], the guaranteed gain and phase margin bounds:

$$GM \in [0.346, 3.618]$$

$$PM \geq \pm 2 \sin^{-1} \left( \frac{1}{2 \times 1.53} \right) = \pm 38^\circ.$$

Taking into account their conservatism, these bounds indicate reasonable robustness margins.

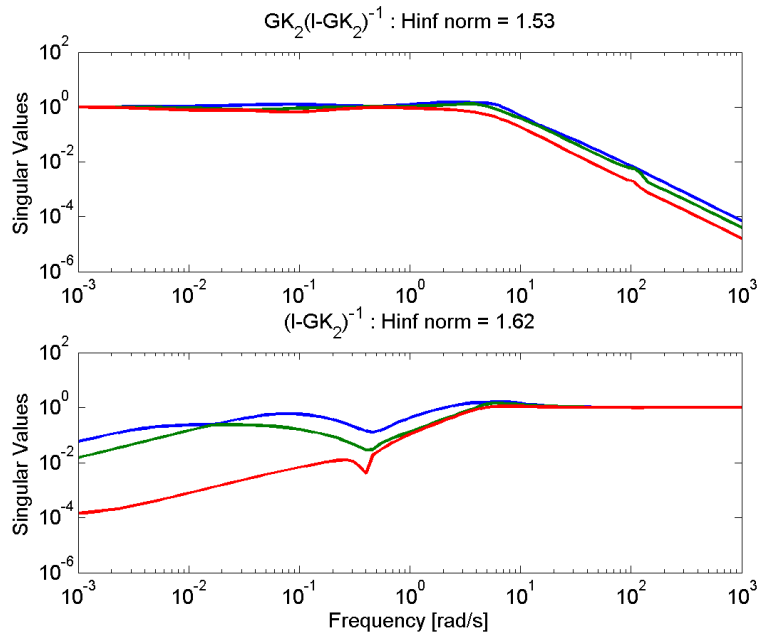


Fig. 8. Input Co-Sensitivity and Sensitivity Singular Value Bode Plots

## 7 NONLINEAR SIMULATIONS

The longitudinal and lateral-direction controllers were then implemented on the FXV-15 nonlinear model. The response of the system to pulse demands of each control axis in turn, at hover and at 40 knots, are shown in Figs. 9-14. The responses are largely as predicted by the linear model. The degradation at 40 knots is relatively small. The control deflections have not been limited in the simulations and it can be seen in Figs. 11 and 12 that the pitch axis controller is using large amounts of longitudinal cyclic to achieve the manoeuvres. The Bell XV-15 had approximately +/- 10 deg of longitudinal cyclic travel.

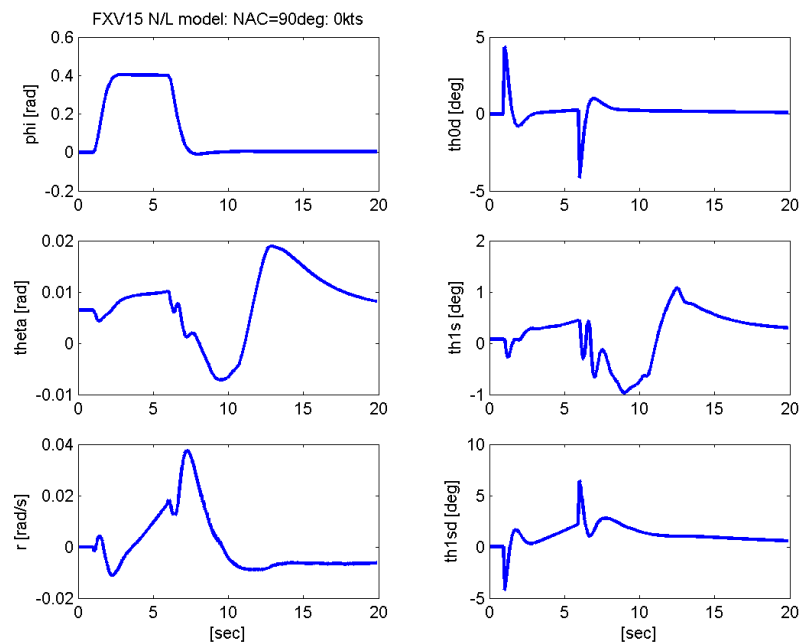


Fig. 9. H-infinity Controller Nonlinear Response Lateral Input (Hover)



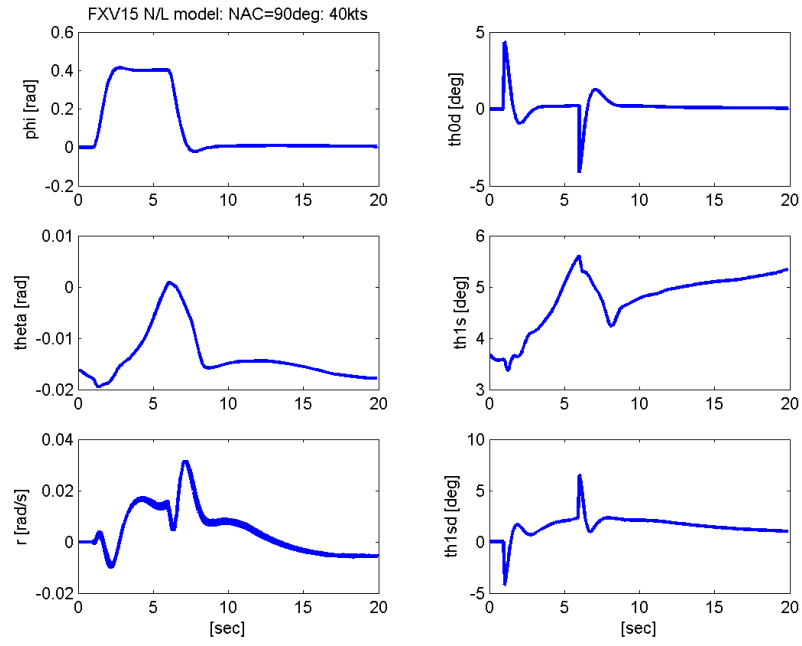


Fig. 10. H-infinity Controller Nonlinear Response to Lateral Input (40kts)

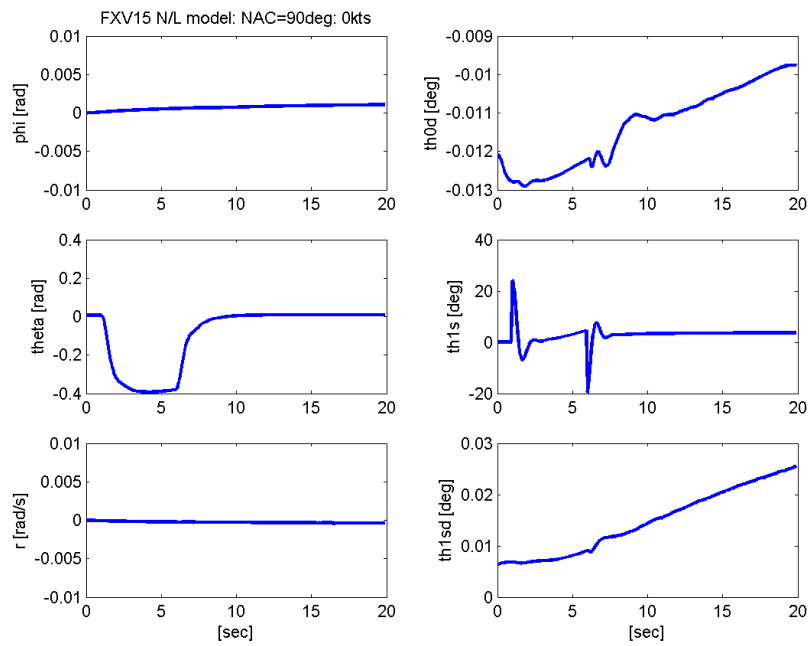


Fig. 11. H-infinity Controller Nonlinear Response to Longitudinal Input (0kts)

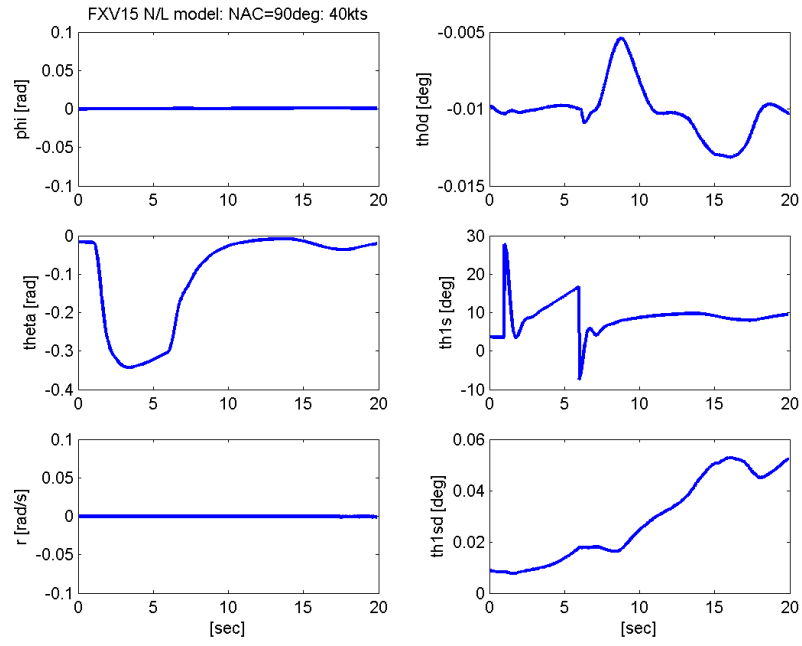


Fig. 12. H-infinity Controller Nonlinear Response to Longitudinal Input (40kts)

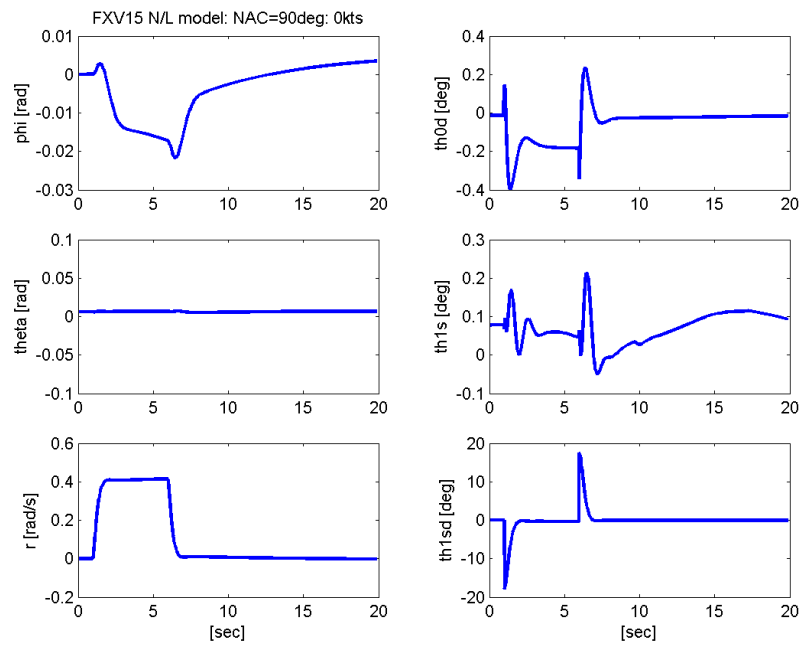


Fig. 13. H-infinity Controller Nonlinear Response to Pedal Input (0kts)

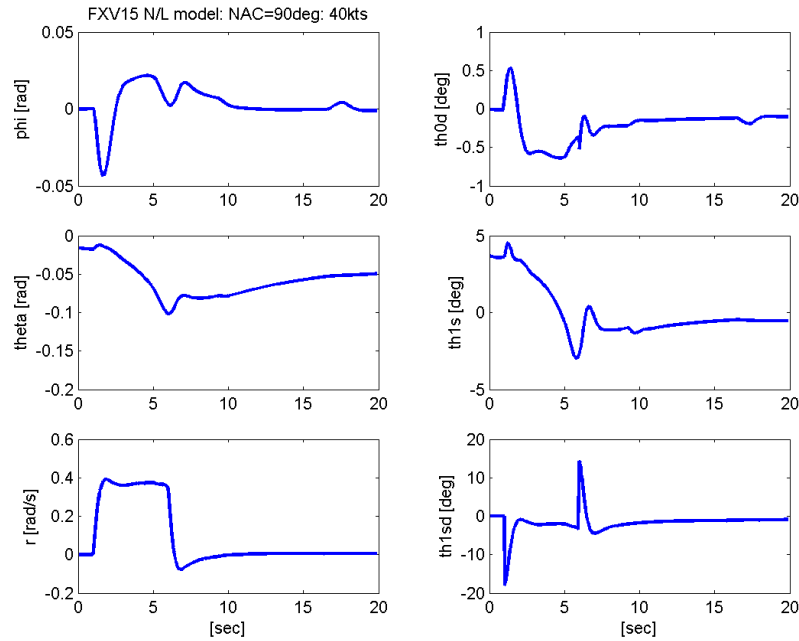


Fig. 14. H-infinity Controller Nonlinear Response to Pedal Input (40kts)

## 8 HANDLING QUALITIES

An analysis of the predicted HQs of the H-infinity control law has been undertaken. Predicted handling qualities derived in accordance with ADS-33, as well as some traditional control criteria such as rise time, settling time etc are now presented. Where appropriate, comparisons are made with the original XV-15 SCAS.

### 8.1 Short Term Frequency Response

The small-amplitude short-term frequency response Bandwidth and Phase-Delay parameters defined in the specification [6] were computed for roll and pitch axes using the high-order linearizations. The results are plotted in Fig. 15 with HQ boundaries for target acquisition and tracking Mission Task Elements (MTEs) from [6] superimposed. The predicted parameters lie well within the Level 1 region. These frequency response parameters were computed directly using linear methods, i.e. higher-order model including gimbal and linear actuator dynamics.

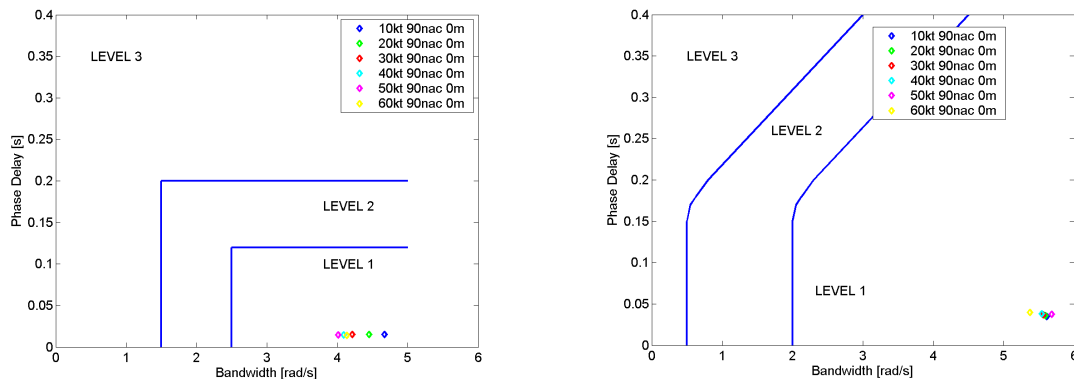


Fig. 15. Short-Term Frequency Response Parameters: (Linear Model)

The bandwidth and phase delay of both the original SCAS and the H-infinity controller were then estimated from the nonlinear FLIGHTLAB simulation model via Fourier analysis of frequency sweeps applied to each control axis in turn. The response of the new control law at 10 knots is shown in Fig. 16. From such time histories, gain, phase and coherence are first estimated. Then, based on these, handling qualities bandwidth and phase delay are determined. The results for the SCAS are shown in Fig. 17, although it should be noted that in this particular case, the time history was obtained by connecting a non-linear model of the SCAS to the high-order *linear* model of the XV-15.

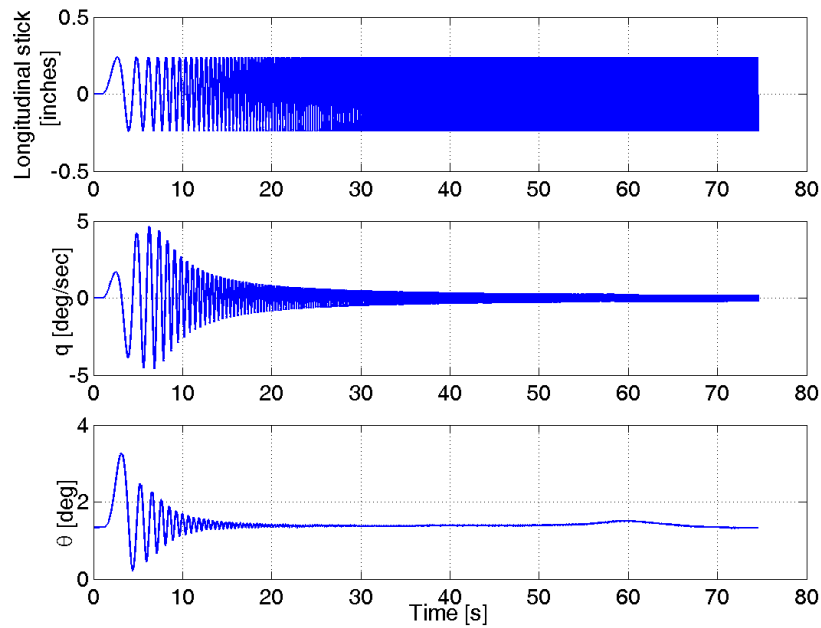


Fig. 16: H-infinity Controller Longitudinal Frequency Sweep, N/L Simulation Model 10 knots

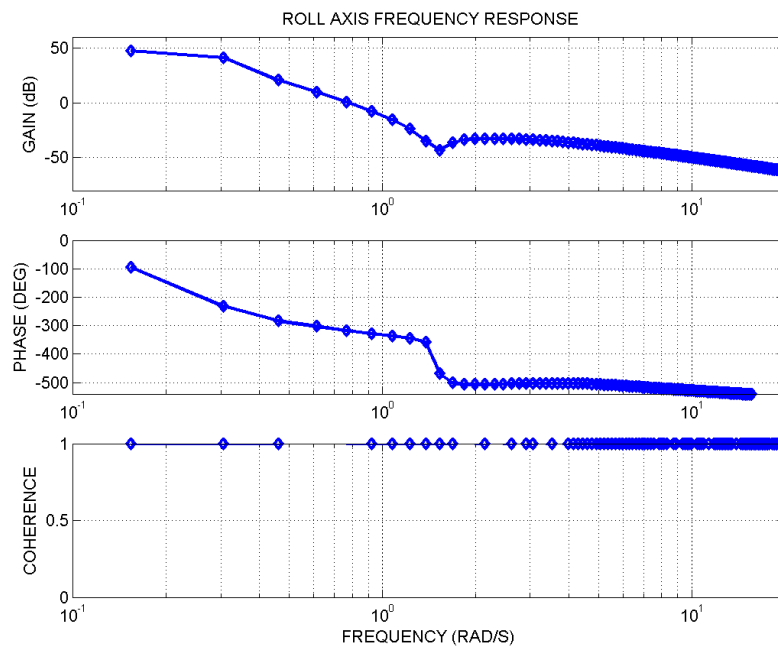


Fig. 17 Roll Axis Frequency Response Estimated with XV-15 SCAS

The bandwidth and phase delay comparison at 10 knots forward flight is summarized in Table 1. The bandwidth of the H-infinity controller is much higher than that of the original SCAS in all axes, resulting in Level 1 predicted handling qualities for combat manoeuvres.

Controller	$\omega_{BW}$ [rad/s]	$\tau_p$ [sec]	Level	
			Combat	Other
<b>Pitch</b>				
SCAS	0.86	0.025	2	2
H-inf	6.1	0.011	1	1
<b>Roll</b>				
SCAS	0.57	0.014	3	2
H-inf	4.9	0.033	1	1
<b>Yaw</b>				
SCAS	0.83	0.031	3	2
H-inf	3.6	0.0082	1	1

Table 1: Bandwidth and phase delay of the FXV-15 at 10 knots forward flight

## 8.2 Quickness

Quickness in pitch and roll was calculated for both control laws using the nonlinear FLIGHTLAB simulation model. The results are summarized in Fig. 18. The pitch attitude quickness of the original SCAS is higher than that of the H-infinity controller (FCL001) for pitch attitude changes smaller than approximately 20 degrees. The same is true for the roll attitude quickness. The different response types of the control laws partly explains the different shapes of the attitude quickness curves. The predicted handling qualities with respect to attitude quickness are summarized in Table 2.

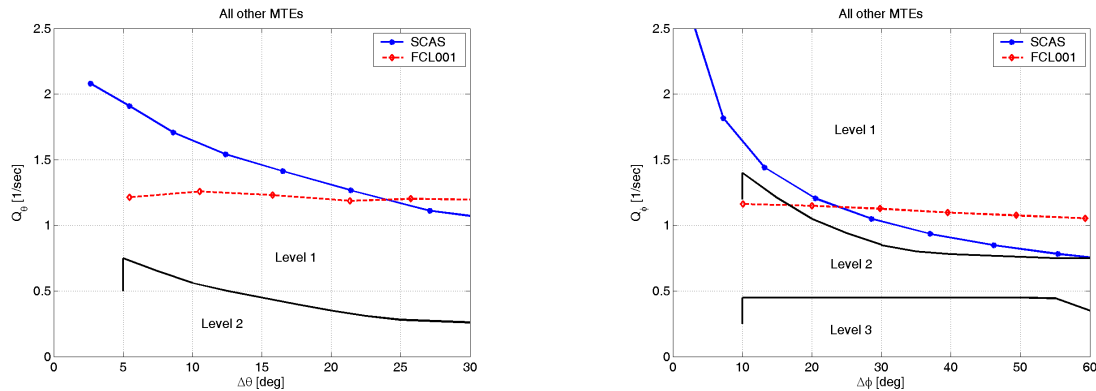


Fig. 18: Attitude quickness comparison at 10 knots forward flight: pitch and roll

Controller	Handling Quality	
	Combat	Other
<b>Pitch</b>		
SCAS	1	1
H-inf	1,2	1
<b>Roll</b>		
SCAS	3	1
H-inf	1,2,3	1,2

Table 2: Attitude quickness at 10 knots forward flight

## 9 PILOTED SIMULATION

The FXV-15 model with H-infinity control law was then ported to the real-time computer system on the advanced flight simulator at Liverpool University [10]. There it was subjected to evaluation by a test-pilot. The pilot was very familiar with the characteristics of the FXV-15 model and its basic SCAS, having tested them on many occasions in the advanced flight simulator. He immediately commented on how stable the H-infinity system was around the hover: so stable that he actually asked for confirmation that he was indeed ‘flying’ the FXV-15 model. He remarked that he had not previously encountered an FXV-15 configuration that “stood still” in the hover with hands off the controls. Two ADS-33 MTEs were tested: the *acceleration-deceleration* and the *sidestep*. The pilot gave Handling Quality Ratings (HQRs) using the Cooper-Harper Scale. Pilot comments were as follows.

### 9.1 Acceleration-deceleration

The primary pitch axis response was predictable and the rate achieved reasonably good. Some pitch and roll to yaw coupling was observed. Other comments included: one and a half seconds to select power; speed up to 50kts. Simulator field-of-view issues at 30 degrees of pitch. One slight overshoot on pitch. There is a lot of power. Key issues: 25 degrees nose down, very aggressive acceleration. Desired performance achieved; Lateral track within 10ft and heading within 10 degrees. Quite pleasant compared to other XV-15 configurations.

#### HQR 3

Data from one of the acceleration-deceleration manoeuvres are shown in Fig.19 and Fig. 20. These show that the workload is largely confined to the longitudinal axis. A measure of the cross-coupling can also be gained.

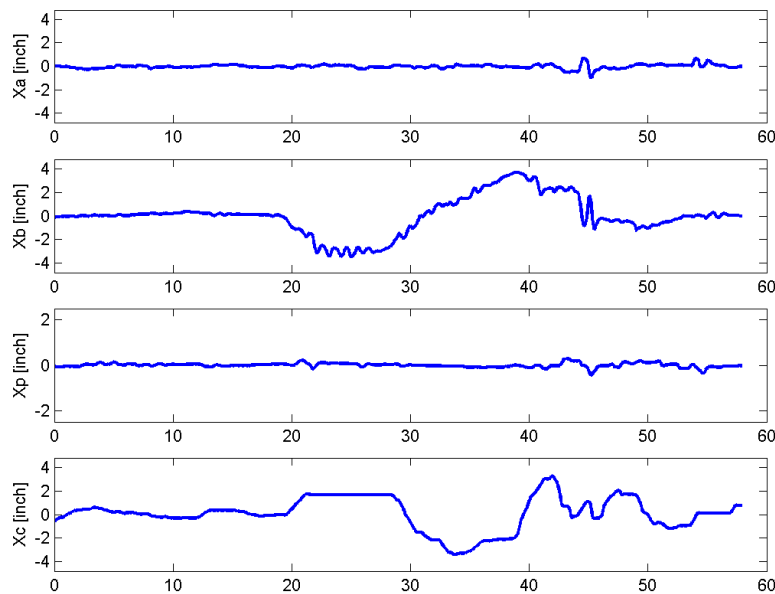


Fig. 19: H-infinity Controller Piloted Accel-Decel Manoeuvre: Stick Inputs

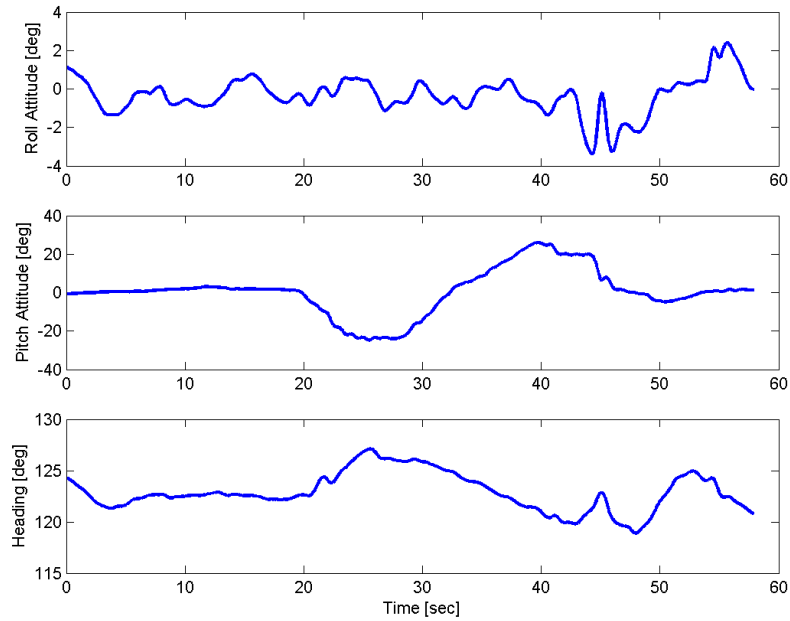


Fig. 20: H-infinity Controller Piloted Accel-Decel Manoeuvre: Euler Angles

## 9.2 Side-step

Speed: up to 35kts; 25 degrees of bank; pitches down and yaws right; cross-coupling quite obtrusive, requires three-axis input; roll-to-yaw cross coupling quite hard to deal with, partly due to pedal sensitivity; large right stick, with left pedal to overcome right yaw; stabilized hover achieved within 5 seconds; objectionable deficiencies, multi-axis input, but flew very well; not like other XV-15 configurations; very impressed with level of stability around trim point. **HQR 4**

The pilot later flew the same manoeuvres with the XV-15 baseline SCAS. The HQRs are summarized in Table 3.

MTE	Control law	HQR
accel-decel	H-INF	3
accel-decel	SCAS	4
Sidestep	H-INF	4
Sidestep	SCAS	6

Table 3: Piloted simulation comparison of H-INF and original SCAS

## 10 CONCLUSIONS

The preliminary analysis presented in this paper indicates that the new H-infinity controller has robustly stabilized the nonlinear model of the Bell XV-15 over a wide part of the low-speed flight envelope. The new system provides an effective attitude command, attitude hold response type in pitch and roll axes satisfying a number of Level 1 frequency response and mid-term eigenvalue-based predicted handling qualities criteria. It represents a significant improvement over the core SCAS in certain key respects.

However, it should be borne in mind that the H-infinity control law has been designed to operate over only a limited part of the envelope, unlike the original XV-15 SCAS, which has a far more complex role to fulfill. The SCAS is a complex system involving gain scheduling which is able to operate over the full envelope of the aircraft, making appropriate use of the helicopter and the conventional controls over the full range of nacelle angle and speed. However, our new design gives some indication of the power of the H-infinity method and of the high performance that may well be achievable in the next generation of tilt-rotor aircraft.

## 11 ACKNOWLEDGMENT

This work was part supported by the UK EPSRC under research grant GR/S42354/01.

## 12 REFERENCES

- [1] Meyer, M.A. & Padfield, G.D., "First steps in the development of handling qualities criteria for a civil tilt-rotor". Proc. American Helicopter Society 58th Annual Forum, Montreal, Canada, 2002.
- [2] Padfield, G.D., Meyer, M., "Progress in the Development of Handling Qualities Criteria for a Civil Tilt Rotor", 29th European Rotorcraft Forum, Friedrichshafen, Germany, Sept 2003
- [3] Manimala, B., Padfield, G.D., Walker, D., Naddei, M., Verde, L., Ciniglio, U., Rollet, P., Sandri, F., "Load alleviation in tilt rotor aircraft through active control, modelling and control concepts", *Aeronautical Journal*, v 108, n 1082, April, 2004, p 169-184
- [4] Maisel, M.D., Guilianetti, D.J. and Dugan, D.C. (2000) "The history of the XV-15 tilt rotor research aircraft". NASA Monographs in Aerospace History No. 17, NASA, Washington D.C.
- [5] Harenda, P. B., Joglekar, M. J., Gaffey, T. M., & Marr, R. L., "A Mathematical Model for Real-Time Flight Simulation of the Bell Model 301 Tilt Rotor Research Aircraft," NASA CR-I14614, 1973
- [6] Anon., "Aeronautical Design Standard Performance Specification, Handling Qualities Requirements for Military Rotorcraft" – ADS-33E-PRF – United States Army and Missile Command – Aviation Engineering Directorate – Redstone Arsenal, Alabama, USA
- [7] Walker, D.J., "Multivariable control of the longitudinal and lateral dynamics of a fly-by-wire helicopter", *IFAC Journal of Control Engineering Practice* vol 11/7 pp 781 – 795, 2003.
- [8] Glover, Keith & McFarlane, D., "Robust stabilization of normalized coprime factor plant descriptions with H infinity-bounded uncertainty", *IEEE Transactions on Automatic Control*, v 34, n 8, Aug, 1989, p 821-830
- [9] N. A. Lehtomaki, N. R. Sandell, Jr., and M. Athans, "Robustness Results in Linear-Quadratic Gaussian Based Multivariable Control Designs," *IEEE Trans. on Automat. Contr.*, vol. AC-26, No. 1, pp. 75-92, Feb. 1981.
- [10] Padfield, G.D., White, M.D., Flight Simulation in Academia; HELIFLIGHT in its first year of operation, *The Aeronautical Journal of the Royal Aeronautical Society*, Vol 107, No 1075, Sept 2003



**ERRATA FOR PAPER FM04 “LOW-SPEED CONTROL OF TILT-ROTOR AIRCRAFT USING H-INFINITY” BY D. J. WALKER, M. VOSKUIJL AND B. J. MANIMALA**

**Equations 1 and 2 should read as follow**

$$\frac{\theta}{\theta_{1s}} = \frac{-3.78(s+0.003)(s+0.174)}{(s+0.462)(s+0.211)[-0.38,0.43]} \frac{[\text{deg}]}{[\text{deg}]} \quad (1)$$

$$\frac{\phi}{\theta_{0d}} = \frac{29.7[0.389,0.144]}{(s+0.74)(s-0.069)[-0.11,0.36]} \frac{[\text{deg}]}{[\text{deg}]} \quad (2)$$